

Finite Difference Time Domain (FDTD) Modeling of Implanted Deep Brain Stimulation Electrodes and Brain Tissue

S. R. I. Gabran, *Member, IEEE*, J. H. Saad, M. M. A. Salama, *Fellow, IEEE*, R. R. Mansour, *Fellow, IEEE*

Abstract – This paper demonstrates the electromagnetic modeling and simulation of an implanted Medtronic deep brain stimulation (DBS) electrode using finite difference time domain (FDTD). The model is developed using Empire XCcel and represents the electrode surrounded with brain tissue assuming homogenous and isotropic medium. The model is created to study the parameters influencing the electric field distribution within the tissue in order to provide reference and benchmarking data for DBS and intra-cortical electrode development.

I. INTRODUCTION

Neuro-modulation is an emerging therapeutic technique with a high potential to control and treat central nervous system disorders related to physiologic, pathogenic or traumatic origins. This therapy employs functional electrical stimulation (FES) to deliver a stimulating electric charge to the targeted brain structure through an implanted intra-cortical electrode. These evolving electrotherapeutic techniques provide irreplaceable therapies for several medical conditions including those which regular surgical and chemical therapies fail to treat. Being an emerging technology; neuro-modulation introduces many challenges that are not yet comprehensively identified, characterized and resolved. Deep brain stimulation (DBS) is an application of functional electrical stimulation developed to treat motor disorders (e.g. Parkinson disease and tremors). DBS was developed to provide treatment for motor disorders through the intermittent delivery of electric charge to the *subthalamic nucleus* (STN), this electrotherapeutic procedure exhibited improvements in patients with Parkinson's disease and torsion dystonia [1].

The progress in the development and optimization of these electrotherapeutic techniques require the comprehension of brain response to the electrical stimulation which is manipulated by the electric field distribution within the brain tissue. This motivated the development of simulation models for the implanted Medtronic 3387 DBS electrode (Medtronic Inc, Minneapolis, MN) in order to estimate the electric field distribution in the ambient brain tissue induced by deep brain stimulation patterns. The information elicited from the simulation results will provide reference benchmark data from an FDA approved and

commercially available DBS electrode. This will guide in the design and development of DBS and intra-cortical electrodes as well as optimizing electrode design and pad geometry and layout. Also, the simulation results will supply data required to evaluate the volume of tissue activated (VTA) by stimulation.

This paper introduces FDTD EM model created using Empire XCcel 5.2 (IMST GmbH, Kamp-Lintfort Germany) exploiting its low frequency algorithms together with the embedded human body models. Since FDTD is a time-domain method, therefore single simulation run can cover a wide frequency range to calculate the electric and magnetic field distribution. On the other hand, using finite element method (FEM) requires multiple runs to achieve similar temporal detail.

II. SIMULATION MODEL

A. Finite Difference Time Domain Modeling

FDTD is a time domain computational electrodynamics modeling technique developed for solving time-dependent Maxwell's equations after discretizing the model using central-difference approximations to the space and time partial derivatives. This yields set of finite-difference equations which are solved in a leapfrog manner to evaluate the electric field vector components in a volume of space at a given instant in time followed by solving for the magnetic field vector components in the same spatial volume at the next instant in time.

B. Electrode Modeling

The Medtronic 3387 electrode shown in Fig. 1 is designed for chronic DBS stimulation. It has a cylindrical polymer core encapsulating the wires which feed four equidistant platinum rings on the perimeter of the electrode shaft representing the stimulation pads. The electrode shaft is 1.28 mm in diameter and the length of each ring is 1.5 mm with a thickness of 0.08 mm. Modeling the electrode tip yields very high dense discretization mesh which consumes memory resources due to the limited ability of the FDTD meshing to process complex geometries requiring non Cartesian grids [2]; therefore it was excluded from the electrode model due to its negligible electromagnetic influence.

C. Brain Tissue Modeling

Different materials have specific responses to externally applied electric fields which are expressed by dielectric material properties (permittivity and conductivity). These values are frequency dependant and anisotropic [3]. Also,

Authors are with the Department of Electrical and Computer Engineering, University of Waterloo, Waterloo, Ontario, Canada.
(emails: sgabran@ieee.org; jfhannas@uwaterloo.ca; msalama@hivolt.uwaterloo.ca; rmansour@maxwell.uwaterloo.ca)

they depend on the composition of brain tissue which differs according to the species (rodents, primates and humans). As frequency decreases, conductivity drops and the dielectric constant increases remarkably along the spectrum exhibiting distinct relaxation regions [4-7]. The values for the dielectric properties of brain tissue were extracted from parametric database of biological tissue which was developed based on Gabriel model [6, 8-10].

The brain tissue representing the surrounding medium is modeled as a homogeneous layer of a lossy dielectric with isotropic and frequency independent characteristics disregarding the anatomical details of the brain [11, 12]. The *globus pallidus* (GPi) and STN which are the targets of DBS are mainly composed of gray matter which at 130 Hz has dielectric constant ϵ_r of 2.462847e6 and conductivity σ of 0.16329 S.m⁻¹ [10] as shown in Fig. 2 and Fig. 3.

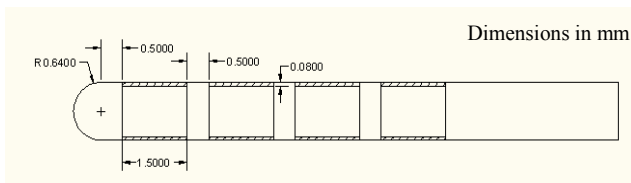


Fig. 1. Medtronic 3387 DBS electrode schematic.

D. Simulation Procedure

The simulation model represents an implanted electrode in a tissue with dimensions 8 x 8 x 12 mm as shown in Fig. 4. Two stimulation pulses were used (Fig. 5): Gaussian pulse representing an approximation to the DBS stimulation pattern to cover wide frequency ranges with a single run, and, monophasic (rectangular) pulse representing the actual pattern [11, 13-15]. The signal was applied as a set of differential voltages fired between the rings. The results are extracted at 130 Hz which corresponds to the fundamental component of a periodic DBS stimulation pattern. To create a finite computational domain, a level 6 perfect matched layer (pml6) is used as an absorbing artificial boundary condition.

III. RESULTS

Simulations were designed to investigate the contribution of different parameters in controlling the distribution of the electric field within the brain tissue. Three main parameters were controlled: firing pattern, permittivity and conductivity. The last two parameters are varied to study the effect of low frequency tissue dielectric properties in shaping the field distribution. The data provided by the simulations is the maximum electric field distribution represents the tissue separated by equipotential contours as shown in Fig. 6, which roughly estimates a volume of tissue activated (VTA) corresponding to a depth of 3 mm.

A. Firing Pattern

Sculpturing the field distribution is required to avoid undesirable activation of untargeted neurons. To investigate

the influence of current steering on sculpturing the electric field, a variable firing pattern was applied using 2 and 3 rings. A constant current source model was used for stimulation, and the weights of the differential currents applied between the rings were controlled to yield different ratios. The electric field distribution for different firing patterns are shown in Fig. 7 exhibiting the flexibility in shaping the field distribution and controlling the VTA as the number of firing rings increases. Single ring firing yields VTA represented in Fig. 7.a, halving the stimulation current level and firing simultaneously from two rings almost double the activated volume as shown in Fig. 7.d.

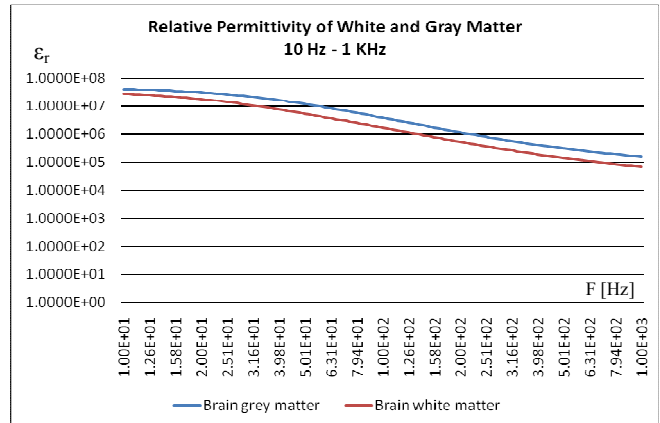


Fig. 2. Semi-log scale of the relative permittivity of white & gray matter 10 Hz - 1 KHz.

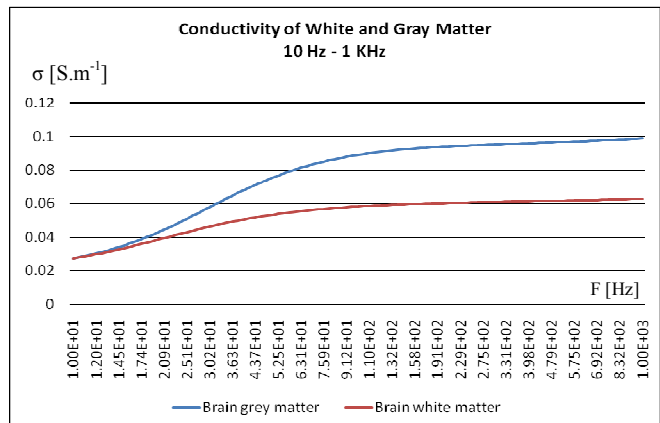


Fig. 3. Conductivity of white & gray matter 10 Hz - 1 KHz.

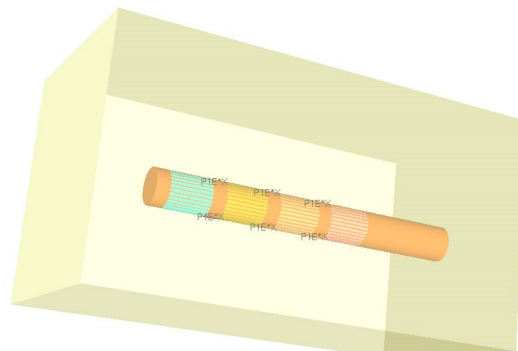


Fig. 4. FDTD simulation model.

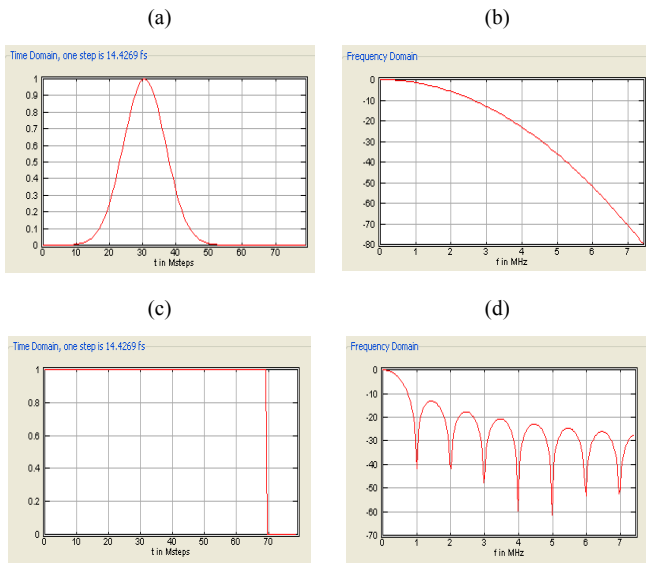


Fig. 5. (a) Time domain Gaussian stimulation pulse, (b) frequency domain of the Gaussian pulse, (c) Time domain monophasic pulse, (d) Monophasic pulse frequency domain.

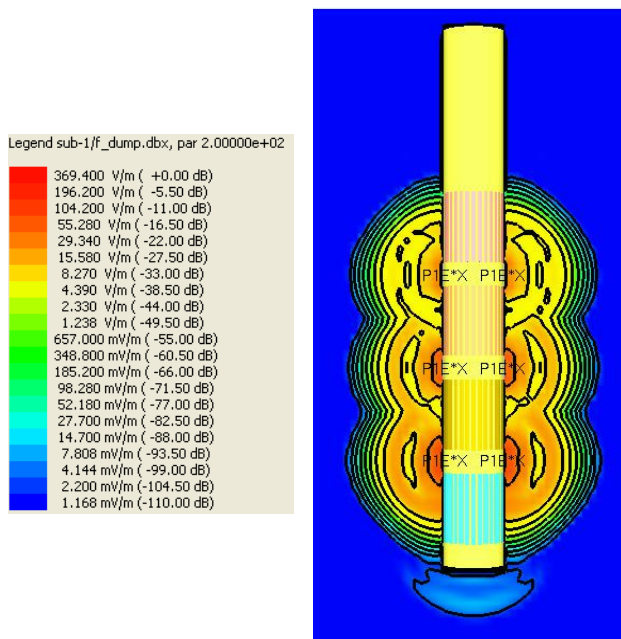


Fig. 6. Electric field distribution for Gaussian pulse, $\epsilon_r = 1e5$, $\sigma = 0.1 \text{ S.m}^{-1}$

B. Tissue Dielectric Properties

The permittivity and conductivity of the tissue were varied to examine the effect of dielectric tissue properties on the distribution of quasi-static electric fields. At very low frequencies ($<1 \text{ KHz}$), tissue responds to the external applied fields as poor conductor, given the remarkable increase in permittivity values and the associated drop in field intensity. The increased permittivity also results in shrinking the VTA, and has more influence on the field distribution than conductivity (Fig. 8 and Fig. 9). Table I demonstrates the maximum values of field intensity for different tissue permittivity values at specific conductivity. Consequently,

the field intensity can be controlled by the stimulation pulse frequency which in turn affects the tissue permittivity.

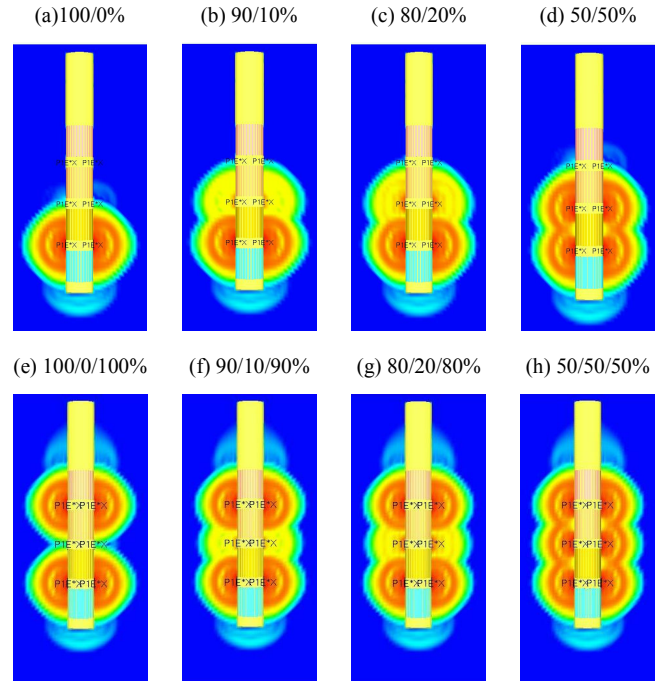


Fig. 7. Current steering and field shaping, upper figures: 2 rings firing, lower figures: 3 rings firing

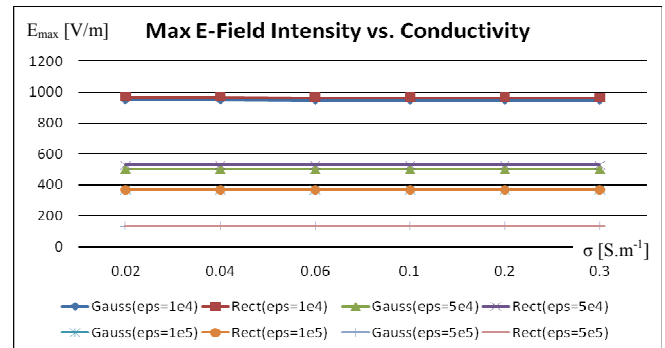


Fig. 8. Maximum electric field values for different permittivities estimated for several conductivities.

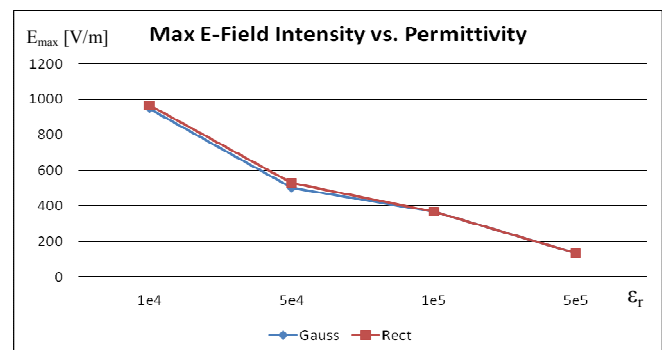


Fig. 9. Electric field intensity vs. permittivity @ $\sigma = 0.1 \text{ S.m}^{-1}$

C. Electrode Array

Electrode arrays provide better access to brain structures and have a potential to enhance the precision of charge delivery to the targeted regions. A multi-shaft electrode array with 4 mm inter-electrode distance was modeled and simulated (Fig. 10). The results emphasized the improved flexibility provided by electrode arrays in controlling field distribution.

TABLE I
MAXIMUM ELECTRIC FIELD INTENSITY [V/m] FOR DIFFERENT TISSUE DIELECTRIC PROPERTIES

Stimulation Pulse and Permittivity	Conductivity					
	0.02	0.04	0.06	0.1	0.2	0.3
Gauss $\epsilon_r = 1e4$	948	948	946	946	946	946
Monophasic $\epsilon_r = 1e4$	968	968	967	967	967	966
Gauss $\epsilon_r = 5e4$	502	502	502	502	502	502
Monophasic $\epsilon_r = 5e4$	529	529	529	529	529	529
Gauss $\epsilon_r = 1e5$	369	369	369	369	369	369
Monophasic $\epsilon_r = 1e5$	370	370	370	370	370	370
Gauss $\epsilon_r = 5e5$	134	134	134	134	134	134
Monophasic $\epsilon_r = 5e5$	135	135	135	135	135	135

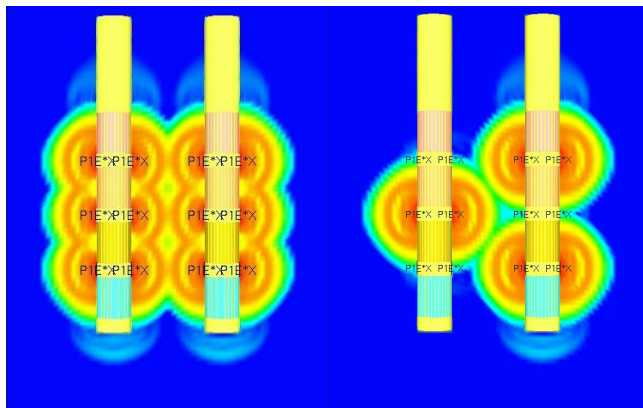


Fig. 10. Two shaft electrode array, left: 100% current level on all rings, right: 0-100-0% (left shaft), 100-0-100% (right shaft).

IV. CONCLUSION

The objective of this research is to create an FDTD model of an implanted DBS electrode and provide reference data for developing DBS and intra-cortical electrodes. Low frequency homogenous model representing the Medtronic 3387 DBS electrode implanted in the STN (represented as human gray matter tissue) was developed based on Gabriel model. The study investigated the effects of several parameters in controlling the volume of tissue activated and improving the spatial precision of charge delivery. This

involved manipulating firing patterns, ratio of differential signals at rings and firing location. Two shaft electrode array was modeled to explore the flexibility and in targeting brain tissue in the STN. In conclusion, the results exhibit the capability of controlling the field distribution to conform to the anatomic target of the stimulation and thus minimizing the stimulation of undesired brain structures.

REFERENCES

- [1] N. P. Bechtereva, A. N. Bondartchuk, V. M. Smirnov, L. A. Meliutcheva, A. N. Shandurina, "Method Of Electrostimulation Of The Deep Brain Structures In Treatment Of Some Chronic Diseases". *Applied Neurophysiology*, vol. 37, pp: 136 – 140, 1975.
- [2] A. Bondeson, T. Rylander, P. Ingelström, "Computational electromagnetics", Springer, 2005.
- [3] L. A. Geddes and L. E. Baker, "The specific resistance of biological material - A compendium of data for the biomedical engineer and physiologist", *Journal of Medical and Biological Engineering and Computing*, vol. 5, No. 3, pp: 271 – 293, May 1967.
- [4] J. G. Stinstra M.J. Peters, "The volume conductor may act as a temporal filter on the ECG and EEG", *Medical and Biological Engineering and Computing*, Springer Berlin / Heidelberg, vol. 36, Number 6, pp: 711 – 716, November 1998.
- [5] H. P. Schwan, "Dielectric Properties of Biological Tissue and Physical Mechanisms of Electromagnetic Field Interaction", *Biological Effects of Nonionizing Radiation*, ACS Symposium Series 157, Karl H. Illinger, the American Chemical Society, 1981.
- [6] F. S. Barnes and B. Greenbaum, "Bioengineering and Biophysical Aspect of Electromagnetic Fields", Taylor and Francis, 2007.
- [7] S. Gabriel, R. W. Lau, C. Gabriel, "The dielectric properties of biological tissues: III. Parametric models for the dielectric spectrum of tissues", vol. 41, No. 11, pp: 2271 – 2293, November 1996.
- [8] C. Gabriel, S. Gabriel, E. Corthout, "The dielectric properties of biological tissues: I. Literature survey", *Physics in medicine and biology*, vol. 41, pp: 2231 – 2249, November 1996.
- [9] S. Gabriel, R. W. Lau, C. Gabriel, "The dielectric properties of biological tissues: II. Measurements in the frequency range 10 Hz to 20 GHz", *Physics in medicine and biology*, vol. 41, pp: 2251–2269, 1996.
- [10] Italian national research council, Institute for Applied Physics: <http://niremf.ifac.cnr.it/tissprop>
- [11] C. R. Butson and C. C. McIntyre, "Current Steering To Control The Volume Of Tissue Activated During Deep Brain Stimulation", *Journal Of Brain Stimulation*, vol. 1, pp: 7–15, 2008.
- [12] C. C. McIntyre and W. M. Grill, "Extracellular Stimulation of Central Neurons: Influence of Stimulus Waveform and Frequency on Neuronal Output", *The Journal of Neurophysiology*, vol. 88, no. 4, pp: 1592 – 1604, 2002.
- [13] S. N. Sotiropoulos and P. N. Steinmetz, "Assessing The Direct Effects Of Deep Brain Stimulation Using Embedded Axon Models", *Journal Of Neural Engineering*, pp: 107–119, 2007.
- [14] C. C. McIntyre, S. Mori, D. L. Sherman, N. V. Thakor, J. L. Vitek, "Electric field and stimulating influence generated by deep brain stimulation of the subthalamic nucleus", *Clinical Neurophysiology*, vol. 115, Issue 3, pp: 589 – 595, March 2004.
- [15] E. Moro, R. J. A. Esselink, J. Xie, M. Hommel, A. L. Benabid, P. Pollak, "The Impact On Parkinson's Disease Of Electrical Parameter Settings In STN Stimulation", *Neurology*, vol. 59, pp: 706 – 13, 2002.